Structure Design and Performance Analysis of a 1-kW-Class HTS Wound-Field Synchronous Machine (MT25-Mon-Af-Po1.04-14)

Ji Hyung Kim[a], Chang Ju Hyeon[a], Huu Luong Quach[a], Sang Heon Chae[a], Min Hyeok Kang[a], Eel-Hwan Kim[a], Yong Soo Yoon[b], Jeyull Lee[c], Haeryong Jeon[c], Seunghak Han[c], Young-Gyun Kim[d], Haigun Lee[d], and Ho Min Kim[a*]

[a] Department of Electrical Engineering, Jeju National University, Jeju, S. Korea, [b] Department of Electrical Engineering, Shin Ansan University, Ansan-si, S. Korea

[c] Department of Electrical and Electronic Engineering, Yonsei University, Seoul, S. Korea, [d] Department of Materials Science and Engineering, Korea University, Seoul, S. Korea

hmkim@jejunu.ac.kr

MT25
25th International Conference on Magnet Technology

ABSTRACT

This paper presents electromagnetic parametric design and two dimensional finite element analysis (2-D FEA) results to develop a 1-kW-class high-temperature superconducting wound-field synchronous machine (HTS WFSM). This is a small scale prototype machine to develop the integrated system with HTS rotating machine and HTS contactless rotary excitation device (CRED) that is connected on the same shaft of the rotating machine and charge the HTS coils for rotor field winding by pumping flux with non-contact method. In order to increase economic efficiency in development stage and machine performance for a 1-kW-class HTS WFSM, various salient pole structures on rotor and magnetic materials on both rotor and stator were considered. Using time-transient solver of 2-D FEA, the various key design parameters were investigated and compared by considering different stator winding coil pitch and dimension of salient pole rotor. Then, final 2-D FEA model was determined based on parametric analysis results and its performance analysis were conducted to estimate the various machine characteristics of a 1-kW-class HTS WFSM.

I. INTRODUCTION

A 1-kW-Class high temperature superconducting (HTS) rotating machine was designed to research and fabricate the novel concept for HTS rotating machine in this paper. This novel idea introduces HTS contactless rotary excitation device (CRED) which is often so-called “rotary type flux pump” using magnetic triggered superconducting switch. Structurally, HTS CRED is integrated on the same rotor shaft of rotating machine and can charge the HTS field coils with non-contact method as conceptually shown in Fig.1. Thus, as eliminating slip-ring, brush, current lead and external power source, it fundamentally can solve the adverse effects of power supply system with contact type in conventional HTS rotating machines such as decline of HTS coil’s thermal stability, increase of cryocooler’s cooling load as well as mechanical noise and vibration generated by bilateral contact between power slip-ring and brush.

In this paper, we solely focused on structure design and analysis for a 1-kW-Class HTS wound-field synchronous machine (WFSM) which will be assembled with HTS CRED developed by other research team in this project. A salient pole type and carbon steel, which can help concentration of magnetic flux and hence generate additional output were considered as a rotor structure and material to reduce high cost second-generation (2G) HTS wire length. However, they electromagnetically can give the harmful influences to performance of rotating machine and HTS coils for rotor field winding. Therefore, electromagnetic effects due to changes of salient pole shape on performance characteristics of rotating machine and HTS coils should be carefully investigated.

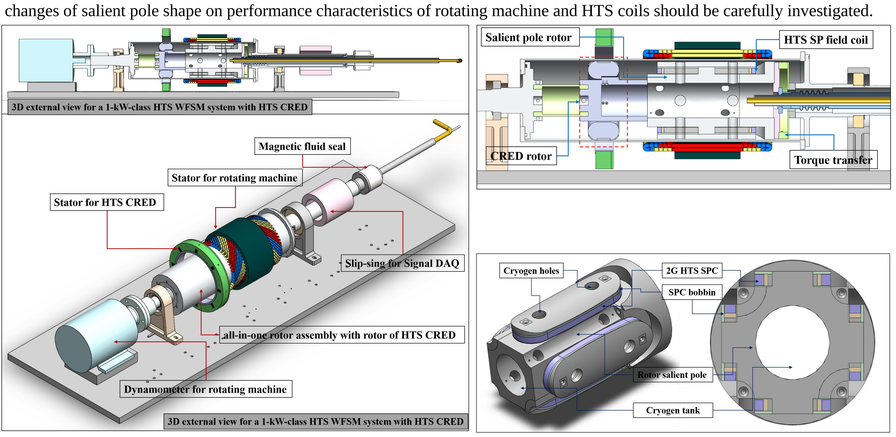

Fig. 1. Conceptual system design view of a 1-kW-class HTS WFSM with a contactless rotary excitation device

II. PARAMETRIC DESIGN OF A 1-KW-CLASS HTS WFSM

A. Preliminary Design of 1-kW-Class WFSM

This iron core is laminated by thin steel plate (50PN470 or S18) along the rotating shaft direction and consists of 48 slots. The four slots are allocated in the number of slots per pole per phase and hence winding turns per phase were distributed in four slots. When choosing commercialized stator core, we consider the volume of cryogen tank inside rotor pole, which can enough store liquid nitrogen (LN2) fed by magnetic fluid seal and cryogen dewar vessel in outside of rotating machine. In addition, carbon steel (SAE-AISI 1045 or S45C) was used as a material of salient pole rotor. HTS field windings were designed by type of race-track and single pan-cake coil (SPC) using SCS 12050 conductor model from SuperPower Inc.

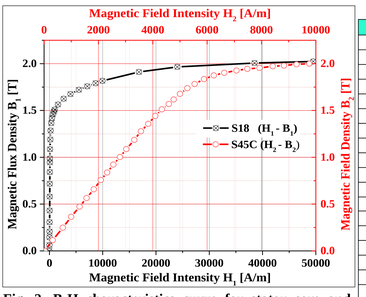

Fig. 2. B-H characteristics curve for stator core and salient pole rotor

TABLE I. DESIGN PARAMETER SPECIFICATIONS OF A 1-KW-CLASS HTS WFSM

Parameters	Unit	Value
Rated/max. power	[kW]	1/2
Rated/max. torque	[Nm]	23.9
Rated rotating speed	[rpm]	400
Rotor pole number	-	4
Rated/max. stator current	[Arms]	4/8
Rated/max. stator current density	[A/mm2]	1.88/3.76
Number of slots	-	48
Pole pitch	-	12
Stator coil number per slot/phase	-	52/416
Fill factor of stator slot	[%]	58
2G HTS conductor	-	SCS 12050
Width/ thickness of conductor	[mm]	12/0.1
Operating field winding current	[A]	30
Overall rotor current density	[A/mm2]	14.7
Field coil inductance	[mH]	≤35
Winding turns per field pole	-	60
Coil type	-	Race-track SPC
Winding type	-	MIT† insulated co-winding
Operating temperature	[K]	77
Cooling method	-	LN2 batch

†: Metal insulator transition

B. Parametric Analysis of Stator Winding Coil Pitch

We analyzed the effects of the application of fractional-pitch winding to reduce spatial harmonics components, which is caused by structural characteristics of teeth and slots in magnetic core. Induced EMF (E_i) and machine input (P_{in}) was inversely proportional to increase of coil pitches. Moreover, copper loss (P_c) together decrease due to reduction of copper length in end winding. VTHDs of E_b for all coil pitches were generally lower because stator core was not saturated by low field excitation. 10/12 coil pitch was suitable stator coil pitches in terms of torque ripple (T_{rc}) characteristic and its VTHD and T_{rc} were 1.19% and 2.29%, respectively.

TABLE II. PARAMETRIC ANALYSIS RESULTS CONSIDERING STATOR COIL PITCHES

Coil Pitches		8/12# (2/3)	9/12# (3/4)	10/12# (5/6)	11/12#	12/12##
Items	Unit	Values				
No-Load Operation Analysis						
E_i	V_{rms}	92.27	98.40	102.87	105.61	106.60
VTHD	%	3.26	1.78	1.09	2.55	3.33
R_a	Ω	2.51	2.66	2.81	2.96	3.11
P_c	W	120.6	127.7	134.9	142.0	149.2
I_a	A_{rms}	4	4	4	4	4
P_{in}	W	1107.3	1180.8	1234.4	1267.3	1279.2
P_{out}	W	986.7	1053.1	1099.6	1125.3	1130.0
η	%	89.11	89.18	89.07	88.79	88.34
Load Operation Analysis						
VTHD†	%	3.38	1.84	1.19	2.70	3.53
T_r	Nm	26.30	28.06	29.35	30.12	30.38
T_c	Nm	2.23	1.33	0.67	1.88	2.53
T_{rc}	%	8.47	4.75	2.29	6.23	8.33

#: Fractional-pitch winding, ##: full-pitch winding, †: without 3rd harmonics

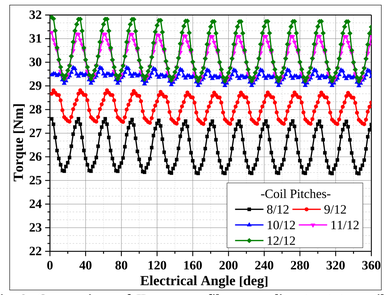

Fig. 3. Comparison of Torque profiles according to stator coil pitches

C. Parametric Analysis of Salient Pole Shapes

The suitable dimension sizes for pole leg width (W_l), pole leg height (H_l), and pole shoe width (W_s) of salient pole have to be selected by parametric analysis. the pole shoe thickness (H_s) at shoe end decides maximum air-gap length (G_{max}) at end of pole arc. As getting shorter Hs, G_{max} is increased and hence air-gap shape is unbalanced along the pole face arc. Note that reference model as shown in Fig. 4 (a) was bullied with W_l 5 of 54.8 mm, H_l 5 of 14 mm, W_s 1 of 77.2 mm, and H_s1 of 4.87 mm, respectively. All parametric models were derived from Fig. 4 (a). All models were modeled and analyzed in time-stepping FEA using ANSYS-Maxwell 2-D 17.2 version. Moreover, motor operation mode with I_{op} of 30 A, rated armature current (I_a) of 4 A_{rms}, and N_s of 400 rpm was simulated with the finite element of about 69000.

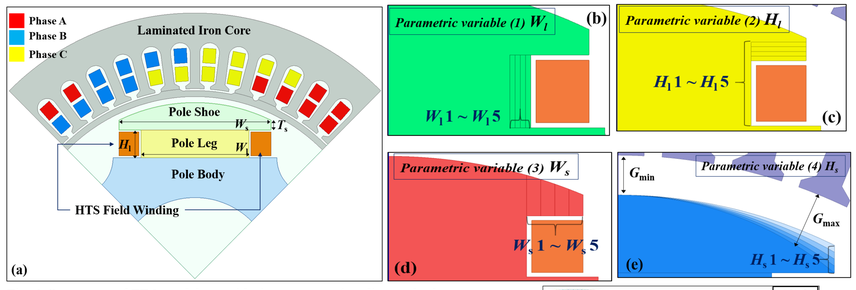

Fig. 4. Structures of FEA models considering parametric salient pole shapes

TABLE III. PARAMETRIC ANALYSIS RESULTS CONSIDERING SALIENT POLE SHAPES

Valua-bles	Values [mm]	Machine Parameter Values					
Parametric valuable (1) W_l							
		E_i# [V_{rms}]	THD# [%]	B_p## [T]	L_f## [mH]	T_r## [Nm]	T_{rc} ## [%]
W_l 1	54.8	102.9	1.088	0.308	37.98	29.35	2.29
Wl 2	52.8	102.7	1.082	0.310	37.93	29.30	2.3
Wl 3	50.8	102.5	1.08	0.310	37.84	29.24	2.29
Wl 4	48.8	102.3	1.08	0.308	37.75	29.18	2.29
Wl 5	46.8	102.1	1.078	0.308	37.65	29.11	2.29
Parametric valuable (2) H_l							
Hl 1	18	102.1	1.291	0.184	36.27	28.94	2.43
Hl 2	17	102.0	1.224	0.198	36.74	29.08	2.41
Hl 3	16	102.4	1.169	0.217	37.17	29.19	2.39
Hl 4	15	102.7	1.123	0.247	37.58	29.28	2.35
Hl 5	14	102.9	1.088	0.308	37.98	29.35	2.29
Parametric valuable (3) W_s							
Ws 1	77.2	102.9	1.088	0.308	37.98	29.35	2.34
W_s 2	71.6	99.53	1.357	0.297	35.50	28.38	2.62
W_s 3	66	96.36	1.434	0.254	33.04	27.29	3.19
W_s 4	60.4	91.90	1.281	0.210	30.76	26.11	2.49
W_s 5	54.8	87.85	0.951	0.172	28.72	24.88	2.29
Parametric valuable (4) H_s							
H_s 1	4.87	102.9	1.088	0.308	37.98	29.35	2.29
H_s 2	3.65	98.56	0.853	0.314	36.30	28.12	1.75
H_s 3	2.43	94.86	0.691	0.324	34.84	27.06	1.34
H_s 4	1.21	91.70	0.573	0.343	33.55	26.15	1.03
H_s 5	0	88.89	0.492	0.384	32.29	25.34	0.81

#: No load operation, ##: load operation

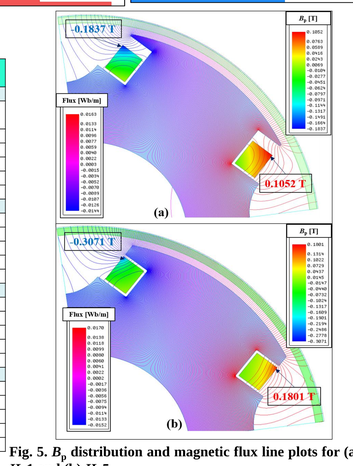

Fig. 5. B_p distribution and magnetic flux line plots for (a) H_l 1 and (b) H_l 5

The effects of H_l’ changes which determine the gap between HTS SPC and bottom of salient pole shoe (g_s) on B_p characteristic of HTS SPC were observed. As getting shorter H_l from 18 to 14 mm, B_p values were increased with ranges from 0.184 to 0.308 T because g_s values should be together shorten as getting shorter H_l and hence highly concentrated magnetic flux across the pole shoe perpendicularly passes and influences on upper area of HTS SPC adjacent to pole shoe as shown in Fig. 5. Moreover, notable changes for other machine parameters without B_p were not observed.

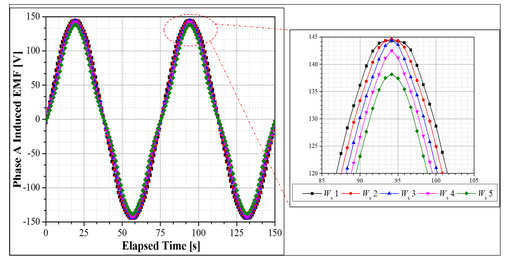

Fig. 6. Comparison of phase A induced EMF waves according to W_s values

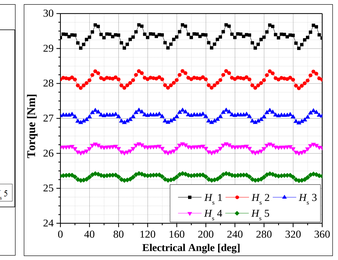

Fig. 7. Comparison of Torque profiles according to H_s values

For reviewing analysis results according to changes of W_s, root mean square (RMS) values for E_i corresponding to each W_s were decreased from 102.9 to 87.85 V_{rms}, respectively. As a results for W_s 1 to W_s 3, as getting shorter W_s, the maximum value of E_i was increased but RMS value of E_i was decreased as shown in Fig. 6 because linkage flux was concentrated at pole shoe center and leaked at end of shortened pole shoe. Moreover, B_p and L_f values were decreased as getting shorter W_s due to same reason in case of effects of H_l changes above explained.

Finally, effects of H_s changes on machine characteristics were investigated. As a getting shorter H_s value of shoe end, air-gap length between stator teeth’ end and shoe face of salient pole is getting unbalanced and that means the shapes of magnetic flux wave in radial direction are changed from square wave to sinusoidal wave because leakage flux was increased by shortened H_s at pole shoe ends. Thus, linkage flux or EMF waveforms are much closer to sinusoidal waveform. The characteristics of VTHDs and T_{rc} were getting superior with decrease of H_s due to above explained reason. However, the magnitudes of E_i and T_r were reduced by decrease of H_s as shown in Fig. 7 due to larger air-gap length, namely, higher magnetic reluctance at shoe ends.

III. MACHINE PERFORMANCE ANALYSIS

A. Performance Analysis of Optimized model in Steady State Motor Operation

The magnitudes of W_l, H_l, W_s, and H_s were chosen as 46.8, 16, 77.2 and 1.21 mm, respectively with consideration of parameter specification as listed in Table I. We conclude that although E_i and T_r of optimal model were about 7% lower than that of reference model, other parameters, viz, characteristics of T_{rc}, B_p, and L_f of optimal model were enhanced and more outstanding than that of reference model in terms of vibration and noise of machine, stability of HTS coil operation, and smooth excitation of HTS coil fed by HTS CRED, respectively. The calculated K_E and K_T of optimal model were 2.28 V_{rms}/rad/s and 6.84 Nm/A_{rms}, respectively. The characteristics of T_r and T_{rc} according to various current phase angle (β) was analyzed to generate maximum torque with constant I_a. The maximum torques for both cases of 4 and 8 A_{rms} armature current were generated at β values of –10° and –20° and torque magnitudes were 27.87 and 58.61 Nm, respectively. However, Torque ripples were minimized at above β values for MTPA control.

TABLE IV. COMPARISON ANALYSIS RESULTS CONSIDERING SALIENT POLE SHAPES

Comparison models	Machine Parameter Values					
	E_i# [Vrms]	THD# [%]	B_p## [T]	L_f## [mH]	T_r## [Nm]	T_{rc}## [%]
Reference model	102.9	1.088	0.308	37.98	29.35	2.29
Optimal model	95.72	0.864	0.221	34.51	27.30	1.66

#: No load operation, ##: load operation

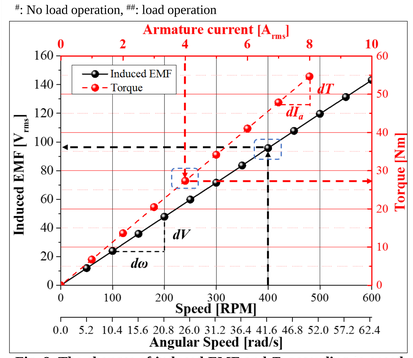

Fig. 8. The changes of induced EMF and T_r according to speed and I_a, respectively

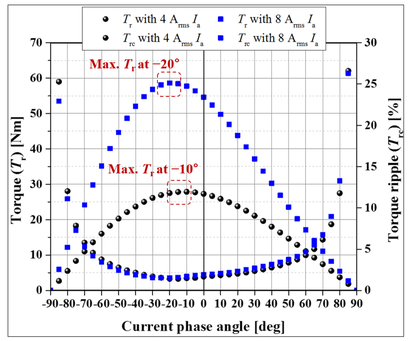

Fig. 9. The changes of T_r and T_{rc} according to various current phase angles

IV. CONCLUSIONS

In this study, a 1-kW-class HTS WFSM was designed and analyzed using 2-D FEM software with consideration of salient pole shape. The key electromagnetic parameter characteristics were investigated by parametric analysis considering various stator winding coil pitches and structural dimensions of salient pole. Then, structurally optimized model was bullied based on parametric analysis results and compared with reference model. In conclusion, the characteristics of Trc, Bp, and Lf of optimal model were enhanced and more outstanding than that of reference model. Finally, various key parameter and machine constants of optimal model as well as β information for MTPA control were investigated in steady-state motor operation to estimate machine performance characteristics. In this paper, we only consider space harmonic component in rotor and stator structure. Thus, for the future study, an operation mode driven by pulse width modulation inverter which can consider time harmonics component should be analyzed to optimize the machine’s torque ripple, losses and efficiency.

Applied Superconductivity Lab. in Department of Electrical Engineering

Jeju National University, Jeju-si, S. Korea

This work was supported by Human Resources Program in Energy Technology of the Korea Institute of Energy Technology Evaluation and Planning (KETEP), granted financial resource from the Ministry of Trade, Industry & Energy, and the National Research Foundation of Korea (NRF) grant funded by the Korea government (MSIP), Republic of Korea. (No. 20164030201230), (No. 2016R1A2B4007324)